Marine Pollution Bulletin 169 (2021) 112517

Contents lists available at ScienceDirect

Marine Pollution Bulletin

journal homepage: www.elsevier.com/locate/marpolbul

# Controlling factors of annual cycle of dimethylsulfide in the Yellow and East China seas

Jia-Wei Shen [a], Liang Zhao [b,*], Hong-Hai Zhang [c,d], Hao Wei [a], Xinyu Guo [e]

[a] School of Marine Science and Technology, Tianjin University, Tianjin 300072, PR China
[b] College of Marine and Environmental Sciences, Tianjin University of Science and Technology, TEDA, Tianjin 300457, PR China
[c] Frontiers Science Center for Deep Ocean Multispheres and Earth System, Key Laboratory of Marine Chemistry Theory and Technology, Ministry of Education, Ocean University of China, Qingdao 266100, PR China
[d] Laboratory of Marine Ecology and Environmental Science, Qingdao National Laboratory for Marine Science and Technology, Qingdao 266237, PR China
[e] Center for Marine Environmental Studies, Ehime University, Matsuyama 790-8577, Japan

ARTICLE INFO

*Keywords:*
Dimethylsulfide
Annual cycle
Ecological model
Marginal sea

ABSTRACT

We developed a dimethylsulfide (DMS) module coupled to an ecological dynamics model studying the annual DMS cycle of the Yellow and East China seas (YECS). The model results showed that surface DMS concentrations ([DMS]) peaked in August along the coast, and there exhibited several DMS peaks offshore annually. In addition, surface [DMS] were higher in the Yellow Sea than that in the East China Sea. The annual mean surface [DMS] of the YECS reached to 4.55 nmol/L, and oceanic DMS emissions from this sea area was 6.78 μmol/($m^2$ day). Several sensitivity experiments demonstrated that phytoplankton community and sea water temperature exerted crucial effects on seasonal variations of surface [DMS]; and phytoplankton community or temperature changed the timing of surface DMS peak while photolysis affected the magnitude of [DMS]. Moreover, the effect size of phytoplankton community or water temperature varied spatially.

## 1. Introduction

Quantitative assessments of climate response to global change induced by human activities, including eutrophication, acidification and global warming, contain many uncertainties, which can be reduced by an improved understanding of biogeochemical feedbacks (Kloster et al., 2006). Marine dimethylsulfide (DMS) is an abundant biogenic volatile sulfur compound mainly originated from dimethylsulfoniopropionate (DMSP). And the transfer of oceanic DMS to the atmosphere is of importance for influencing aerosol formation and cloud albedo over the ocean (Charlson et al., 1987; Fiddes et al., 2018); and future increases of this flux could alleviate warming (Bopp et al., 2004; Gabric et al., 2004; Grandey and Wang, 2015).

Surface DMS concentration and DMS emissions are higher in marginal seas (Kettle et al., 1999; Gypens and Borges, 2014), and changes in surface DMS and its flux under a climate change scenarios vary spatially (Bopp et al., 2004; Kloster et al., 2007). Thus, additional uncertainty may be introduced in assessments of DMS effects on climate if the spatio-temporal variations of DMS level especially in marginal seas, which are involved in complex environmental changes, is not well-researched.

The area encompassing the Yellow and East China seas (YECS) is one of the most extensive marginal sea basins in the western Pacific Ocean. The YECS, which accounts for a small part of the global ocean, contributes greatly to the release of DMS (Yang et al., 2014; Jian et al., 2018; Xu et al., 2019). And a significant relationship between chlorophyll *a* (Chla) and DMS concentrations has been observed, indicating that phytoplankton biomass might play a crucial role in controlling variations in DMS (Yang et al., 2011; Gao et al., 2017; Jian et al., 2018). Some controlled experiments have quantified contributions of different processes to the DMS stock (Jian et al., 2018; Xu et al., 2019; Zhai et al., 2019), and Xu et al. (2019) suggested that both microbial consumption and photooxidation determine the removal of surface DMS.

Observational data contain large spatio-temporal discontinuities (Yang et al., 2011). The relationship between DMS and other factors (Gao et al., 2017; Jian et al., 2018; Shen et al., 2019), and the contribution of each DMS sink (Xu et al., 2019), varies spatially and temporally. Therefore, we still need to deepen our understanding on seasonal and horizontal variations of DMS concentrations and their controlling

* Corresponding author at: College of Marine and Environmental Sciences, Tianjin University of Science and Technology, 29 Thirteenth Avenue, TEDA, Tianjin 300457, PR China.
*E-mail address:* zhaoliang@tust.edu.cn (L. Zhao).

https://doi.org/10.1016/j.marpolbul.2021.112517
Received 6 February 2021; Received in revised form 13 May 2021; Accepted 15 May 2021

factors. In addition to in-situ observations and controlled experiments, numerical modeling is also a tool to understand annual cycle of DMS. And model studies have focused on the marine DMS cycle of some other marginal seas (Gabric et al., 1999; Archer et al., 2002; Gypens et al., 2014). In this study, we developed a DMS module and coupled it to a three-dimensional ecological dynamics model to studying the annual cycle of the YECS climatologic DMS and discussing its controlling factors.

## 2. Model description

We developed a DMS module that included two prognostic variables, DMS and dissolved dimethylsulfoniopropionate (DMSPd, a precursor of DMS), and coupled it to the East China Sea Ecological Model (ECSECOM). The ECSECOM has a hydrodynamic and a biological module and was used to study seasonal variations in nutrients and phytoplankton (Zhao and Guo, 2011), nutrient transport and dynamic (Wang et al., 2019) and role of oceanic and terrestrial nutrients in primary production (Zhang et al., 2019). Water temperature, currents and diffusivity coefficients from the hydrodynamic module, and irradiance and phytoplankton biomass from the biological module were used as inputs to the DMS module.

### 2.1. Hydrodynamic and biological modules

The hydrodynamic module is a nested model of the YECS with a high horizontal resolution (1/18°) derived from the Princeton Ocean Model (Guo et al., 2003). The module has 21 sigma (σ) levels, and its domain covers the YECS with an open boundary along the southern and eastern boundaries (Fig. 1). The time step was 6 s for the external mode and 360 s for the internal mode. Tidal forcing ($M_2$, $S_2$, $K_1$ and $O_1$ tides) were added along the lateral boundary (Wang et al., 2008).

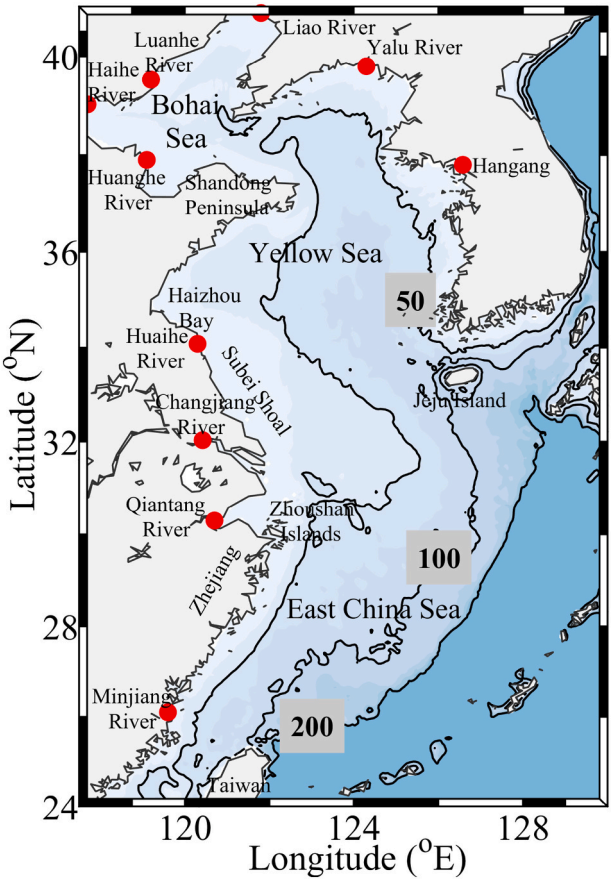


**Fig. 1.** Model domain and bathymetry. Red dots denote rivers along the coastline. Black contours with number denote 50, 100 and 200 m isobaths. (For interpretation of the references to colour in this figure legend, the reader is referred to the web version of this article.)

The biological module developed for the YECS (Zhao and Guo, 2011) is derived from the biological part of the Norwegian Ecological Model system (Skogen and Søiland, 1998). The details of this module are available in Zhao and Guo (2011) and Wang et al. (2019). Some boundary conditions for the biogeochemical variables were adjusted, including nutrient concentrations at the western part of the open southern boundary and atmospheric nitrogen deposition (Wang et al., 2019). To decouple the nutrient cycles of nitrate and phosphate, we categorized the detritus into particulate organic nitrogen and particulate organic phosphorus.

### 2.2. Dimethylsulfide module

We added DMSPd and DMS into the DMS module. The governing equations of DMSPd and DMS in sea water (concentrations in nmol/L) are given in Eqs. (1) and (2), and the parameters ($C_1$ to $C_9$) used in the standard run are provided in Table 1:

$$\frac{\partial(DMSPd)}{\partial(t)} + \underbrace{adv(DMSPd)}_{\text{advection term}} = \underbrace{diff(DMSPd)}_{\text{diffusion term}} + \underbrace{C_1{*}(C_3{*}\mathrm{f}(T){*}P_{DIA} + D_{DIA})}_{\text{phytoplankton active exudation and autolysis}} + \underbrace{C_2{*}(C_4{*}\mathrm{f}(T){*}P_{FLA} + D_{FLA})}_{\text{phytoplankton active exudation and autolysis}} - \underbrace{C_5{*}\mathrm{f}(T){*}DMSPd}_{\text{free DMSP}-\text{lyase cleavage}} - \underbrace{C_6{*}DMSPd}_{\text{microbial DMSPd degradation}} \quad (1)$$

$$\frac{\partial(DMS)}{\partial(t)} + \underbrace{adv(DMS)}_{\text{advection term}} = \underbrace{diff(DMS)}_{\text{diffusion term}} + \underbrace{C_5{*}\mathrm{f}(T){*}DMSPd}_{\text{free DMSP}-\text{lyase cleavage}} + \underbrace{C_7{*}C_6{*}DMSPd}_{\text{microbial DMSP cleavage}} - \underbrace{C_8{*}DMS}_{\text{microbial DMS degradation}} - \underbrace{C_9{*}Iz{*}DMS}_{\text{photolysis}} \quad (2)$$

where adv and diff are advection and diffusion terms of the two prognostic variables, P (mgN/m$^3$) and D (mgN/m$^3$) are phytoplankton biomass stock and stock of dead phytoplankton, respectively, and the subscripts DIA and FLA represent diatoms and flagellates.

We did not consider the DMS flux at the bottom boundary because of the lack of in-situ data. And the sea-to-air DMS flux was specified as the surface boundary condition (Eq. (3)):

$$\frac{K_H}{H}\left(\frac{\partial(DMS)}{\partial\sigma}\right) = -k_{flux}{*}(DMS_{sea} - DMS_{air}) \quad (3)$$

where $K_H$ (m$^2$/s) is the vertical diffusion coefficient, H (m) is the water

**Table 1**
Parameters used in the dimethylsulfide (DMS) module for the standard run.

| Parameter description | Symbol | Value | Unit |
|---|---|---|---|
| Intercellular S(DMSPp): N in a cell of DIA | $C_1$ | 0.30 | mg S/mg N |
| Intercellular S(DMSPp): N in a cell of FLA | $C_2$ | 0.80 | mg S/mg N |
| Active exudation rate constant at 0 degree Celsius for DIA | $C_3$ | 0.034 | 1/day |
| Active exudation rate constant at 0 degree Celsius for FLA | $C_4$ | 0.046 | 1/day |
| Free DMSP-lyase cleavage rate constant at 0 degree Celsius | $C_5$ | 0.18 | 1/day |
| Microbial DMSPd degradation rate constant | $C_6$ | 4.00 | 1/day |
| Proportion of consumed DMSPd cleaved to DMS by microbe | $C_7$ | 0.45 | / |
| Microbial DMS degradation rate constant | $C_8$ | 3.00 | 1/day |
| DMS photochemical oxidation rate per unit of radiation | $C_9$ | 0.0033 | 1/(day·W/m$^2$) |

DMSPp = particulate dimethylsulfoniopropionate; DIA = diatoms; FLA = flagellates; DMSPd = dissolved dimethylsulfoniopropionate.

depth plus sea surface elevation known as total water depth, and $k_{flux}$ (m/s) represents sea-to-air DMS exchange rate. DMS in the air ($DMS_{air}$) was assumed to be 0 nmol/L throughout this study given the results from Zhu et al. (2019).

#### 2.2.1. Sources and sinks of dissolved dimethylsulfoniopropionate

In this module, biological sources of DMSPd included phytoplankton active exudation and autolysis while sinks included free DMSP–lyase cleavage and microbial degradation (Eq. (1)). Phytoplankton active exudation is a pathway where particulate dimethylsulfoniopropionate (DMSPp) in cells can be released into the DMSPd phase. The ratio of intercellular DMSP sulfur to nitrogen (S:N) in a DIA or FLA cell were referred to as $C_1$ and $C_2$; $C_3$ (or $C_4$) is the exudation rate constant of DIA (or FLA) at 0 degree Celsius, and f(T) is a temperature dependent coefficient suggested by Geider et al. (1998), details of this coefficient was provided in Eq. (4). The intercellular S:N of a DIA ($C_1$) is 0.06 ± 0.17 mg S/mg N (Keller et al., 1989), and the intercellular S:N of a FLA ($C_2$) is 0.33 ± 0.48 mg S/mg N (Stefels et al., 2007). For the standard run, $C_1$ and $C_2$ were set to 0.30 and 0.80 mg S/mg N after adjustments which is mainly based on the performance of surface DMS concentrations (Table 1), and following Archer et al. (2002), we set $C_3$ and $C_4$ to 0.034 and 0.046/day (Table 1). Autolysis represents DMSPp released by phytoplankton at death. As for free DMSP-lyase cleavage, Archer et al. (2002) showed that setting for free DMSP–lyase cleavage rate constant was 0.125/day. However, in this manuscript, free DMSP–lyase cleavage shown in Eq. (1) included the cleavage of DMSPd not only by free enzymes or free-living bacteria, but also by phytoplankton intercellular DMSP-lyase, and this cleavage rate constant at 0 degree Celsius ($C_5$) was set to 0.18/day (Table 1). DMSPd can be consumed by microbial communities. Previous studies showed that microbial DMSPd degradation rate constant ($C_6$) of the YECS is 0.91 to 14.10/day (Jian et al., 2018; Xu et al., 2019; Zhai et al., 2019), and it was set to 4.00/day (Table 1).

$$\begin{aligned} f(T) &= e^{0.063*T}, T \leq 30^{\circ}C \\ f(T) &= e^{0.063*30}, T > 30^{\circ}C \end{aligned} \quad (4)$$

#### 2.2.2. Sources and sinks of dimethylsulfide

Sources of marine DMS include free DMSP-lyase cleavage and microbial DMSP–lyase cleavage, and sinks for DMS include microbial DMS degradation, photolysis and air–sea exchange. Microbial DMSP–lyase cleavage is a pathway where DMSPd is consumed by microbes (Stefels et al., 2007). The proportion of consumed DMSPd cleaved to DMS ($C_7$) was assumed to 0.45 (Table 1) based on previous studies that suggested $C_7$ may range from 0.09 to 0.71 with an average of 0.40 of the YECS (Jian et al., 2018; Xu et al., 2019; Zhai et al., 2019). Microbial degradation is usually the main sink of marine DMS (Stefels et al., 2007). And its degradation rate constant ($C_8$) is in the range of 0.14 to 7.53/day in the YECS (Jian et al., 2018; Xu et al., 2019; Zhai et al., 2019), and was set to 3.00/day (Table 1). In this module, the photolysis rate was assumed to be a linear function of incident solar radiation ($I_Z$, W/m$^2$). Some studies showed that it ranges from 0.51 to 3.85/day in the YECS (Jian et al., 2018; Xu et al., 2019), we trebled the photolysis rate per unit of irradiance ($C_9$) gained from Kloster et al. (2006). And $k_{flux}$ (cm/h) was calculated according to Eq. (5) (Nightingale et al., 2000):

$$k_{flux} = \left(0.222*U_{10}{}^2 + 0.333*U_{10}\right)*\left(\frac{Sc(T)}{600}\right)^{-0.5} \quad (5)$$

where $U_{10}$ (m/s) is wind speed at 10 m above sea surface derived from ERA-Interim database (https://www.ecmwf.int/en/forecasts/datasets/reanalysis-datasets/era-interim). *Sc*, the Schmidt number of DMS, is a temperature dependent variable (Saltzman et al., 1993).

### 2.3. Model setup

The concentrations of DMSPd and DMS in river water are relatively low. Therefore, our DMS module did not include riverine inputs of DMSPd or DMS. Lana et al. (2011) provided a global distribution of surface DMS level, which showed that the concentration is 1–2 nmol/L off south of Taiwan and to the east of the Ryukyu Islands. In this study, the DMS and the DMSPd levels along the southern and southeastern open boundaries were set to 1 nmol/L (above 200 m) and 0 nmol/L (under 200 m). YECS DMS concentrations reached stable seasonal values after a spin-up of 3 year, and the model outputs from the fourth year were used for examining the annual cycle of climatologic marine DMS.

Phytoplankton biomass, community and temperature all have an important impact on the marine DMS cycle (Stefels et al., 2007; Yang et al., 2014; Jian et al., 2018; Speeckaert et al., 2018). Hence, several sensitivity experiments were designed to investigate the direct influence of these biogeochemical variables on the seasonality of surface DMS concentrations (Table 2). Run 1 is the standard run including all direct effects. Run 2 does not include the direct effect of phytoplankton community (i.e., two phytoplankton function types (DIA and FLA) have the same intercellular S:N and active exudation rate). To obtain realistic DMS concentrations, we set $C_1$ and $C_2$ ($C_3$ and $C_4$) to 0.50 mg S/mg N (0.034/day) for the Run 2. In Run 3, we eliminated the impact of water temperature on phytoplankton active exudation and free DMSP-lyase cleavage after setting f(T) to 1, moreover, we trebled the $C_3$, $C_4$ and $C_5$ for obtaining a realistic result. Run 4 closed the photolysis term (seen in Eq. (2)), focusing on the direct effect of radiation on the seasonal DMS concentration variations.

### 2.4. Description of in-situ data

We compiled an observational dataset containing in-situ data acquired during 48 survey flights over the YECS between 2005 and 2017 from literatures. In total, surface data were collected from 1885 stations. Large spatio-temporal discontinuities are present in this dataset; for example, more data were collected in July and November (Fig. S1a). To better optimize the model performance, a gridded climatology concentration field of monthly DMS, DMSPd and Chla data (hereafter referred to as YECS_DMS, YECS_DMSPd and YECS_CHL) were constructed based on in-situ dataset (the details of in-situ dataset and gridded climatology are available in the Supplementary Material). Fig. S1b shows monthly climatology grids; lower grid numbers were noted in August and September, which was taken into account when we verified the seasonal cycle.

## 3. Results

### 3.1. Model evaluation

#### 3.1.1. Validation of surface dimethylsulfide concentrations

The horizontal distribution of annual mean surface (at a depth of 2 m) DMS concentrations ([DMS]) from the standard run is shown in Fig. 2a with observational data from the YECS_DMS dataset plotted as small dots arrayed on top of the model result. The small dots indicated

**Table 2**
Settings for the sensitivity experiments used to study the direct impact of phytoplankton community, temperature and radiation on dimethylsulfide cycle.

| Run | $C_1$–$C_4$ affected by PFT | Stress active exudation and free DMSP cleavage | Photolysis |
|---|---|---|---|
| Run 1 | Yes | Yes | Yes |
| Run 2 | No | Yes | Yes |
| Run 3 | Yes | No | Yes |
| Run 4 | Yes | Yes | No |

PFT = phytoplankton function type; DMSP = dimethylsulfoniopropionate.

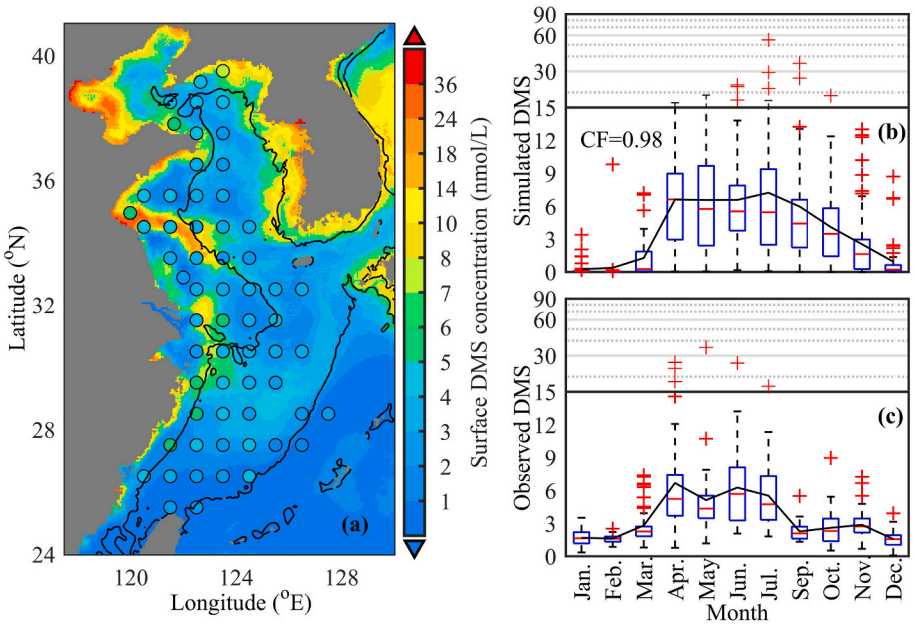


**Fig. 2.** Validation of surface dimethylsulfide (DMS). (**a**) Comparison of annual mean DMS concentrations (nmol/L) for the standard run (contour plot) to the results from the YECS_DMS (colored dots). Black contours denote 50 and 200 m isobaths. Boxplot of DMS concentrations (nmol/L) for the (**b**) gridded model output and (**c**) YECS_DMS. The red lines within each box are the median, the boxes define the hinge (25%–75% quartile), the horizontal lines outside each box are 1.5 times the hinge, and black solid lines provide seasonal variations in the arithmetical mean. The Cost Function (CF) is reported in the literature (Allen et al., 2007; Dabrowski et al., 2014) and its expression is given in Eq. (6). (For interpretation of the references to colour in this figure legend, the reader is referred to the web version of this article.)

higher annual mean surface [DMS] (>5 nmol/L) in the Yalu Estuary, off the coast of northern Shandong Peninsula, Haizhou Bay, east of the Changjiang Estuary, off the coast of Zhejiang and Fujian provinces; surface [DMS] was higher in the coast, and [DMS] was greater in the Yellow Sea (YS) than that in the East China Sea (ECS; Fig. 2a). The distribution of surface DMS level from the model output was consistent with that of the observational data (Fig. 2a). The model output also captured the characteristics of seasonal variation of surface DMS level. Both higher simulated or observed [DMS] occurred between April and July; and [DMS] was higher in autumn as compared to that in winter (Fig. 2b and c). The discrepancy was that we overestimated surface [DMS] of the YS, underestimated [DMS] of the ECS (Fig. 2a); and the model also underestimated it in winter (Fig. 2b and c).

The Cost Function (CF; Eq. (6)) is an evaluating indicator of the goodness of fit, defined as the ratio of mean absolute error (MAE) to the standard deviation of the observational data (Allen et al., 2007; Dabrowski et al., 2014):

$$CF = \frac{\sum|C_S - C_M|}{n^*\sigma_M} \tag{6}$$

where $C_S$ is model result, $C_M$ is observational data, n is data number and $\sigma_M$ is the standard deviation of all observational data. A score of CF < 1 indicates excellent/very good performance; a score of CF = 1–2 indicates good performance; a score of CF = 2–3 indicates reasonable performance; a score of CF > 3 indicates poor/bad performance (Dabrowski et al., 2014).

As far as the performance assessment in modeling DMS based on the CF value is concerned, the MAE was within one $\sigma_M$ (CF = 0.98) meaning that our model output performance was excellent/very good in the YECS. The annual mean surface [DMS] calculated from the YECS_DMS was 3.74 nmol/L, and the model output of the same sea areas reached to 4.18 nmol/L, overestimated by 12% or so. And the annual mean simulated surface DMSPd concentration ([DMSPd]) was also higher than the value derived from the YECS_DMSPd. In general, our model reproduced the spatial and seasonal variations in surface [DMS] of the YECS.

### 3.1.2. *Validation of surface total chlorophyll a concentrations and phytoplankton community structure*

Phytoplankton biomass is an core indicator of marine DMS in the YECS (Yang et al., 2014; Jian et al., 2018). The model performance in simulating surface DIA Chla concentrations ([Chla]) plus FLA [Chla] known as total [Chla] is shown in Fig. 3. The data from the YECS_CHL dataset (small dots) indicated higher annual mean surface [Chla] (>1 μg/L) in the Yalu Estuary and adjacent areas, off the coast of northern Shandong Peninsula, Haizhou Bay, Subei Shoal and the ECS inner shelf; the model output was able to capture these leading features (Fig. 3). And the annual mean surface [Chla] calculated from the YECS_CHL was 0.83 μg/L, and the model output (1.17 μg/L) was relatively higher for the same area; moreover, and it was 1.19 μg/L in the YECS (<200 m water depth), which was close to the locally modified satellite Chla concentrations (1.12 μg/L) provided by Hao et al. (2019). The discrepancy was that the ECSECOM output overestimated annual mean total [Chla] in the YS especially the western 34.5°N transect, resulting in the

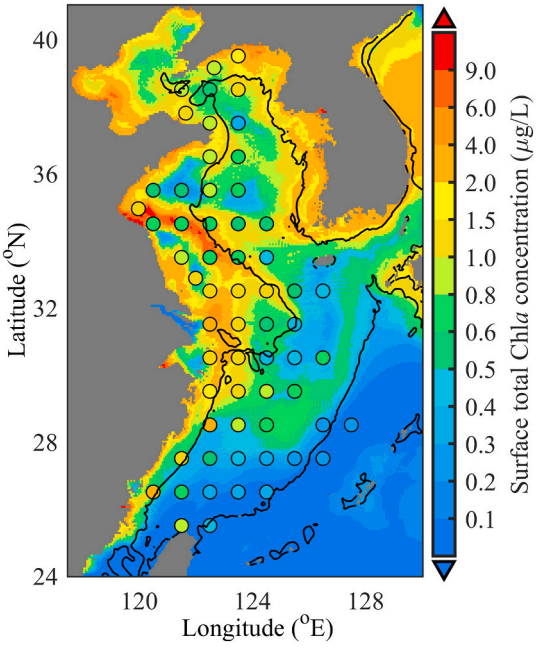


**Fig. 3.** Comparison of annual mean surface concentrations of total chlorophyll *a* (Chla; μg/L) for the standard run (contour plot) to the results from the YECS_CHL (scatter diagram). Black contours denote 50 and 200 m isobaths.

overestimation of [DMSPd], [DMS]; and model output underestimated total [Chla] in the ECS as a whole.

The structure of the phytoplankton community can affect annual patterns of marine [DMS] (Vogt et al., 2010; Speeckaert et al., 2018). So, we also evaluated phytoplankton community here. In nearshore YECS regions (<50 m water depth), annual mean proportion of the DIA [Chla] of which the nearest corresponding satellite-derived data was [Chla] of microphytoplankton, contributed the most to the annual average of total [Chla] (Fig. 4a), whereas FLA [Chla] of which the nearest corresponding satellite-derived data was the summation of nanophytoplankton [Chla] and picophytoplankton [Chla], explained the highest proportion in offshore regions (>50 m water depth; Fig. 4b). This was in better agreement with the results of satellite-derived dataset gained from literatures (Sun et al., 2019a; Sun et al., 2019b).

### 3.2. Annual cycle of surface dimethylsulfide concentrations

The annual mean surface [DMS] arrived at 4.55 nmol/L in the YECS (<200 m water depth; Table 3). And monthly surface [DMS] varied considerably spatially; it decreased from inshore to offshore over the most of the year (Fig. 5). So, a quantitative analysis of the annual cycle of surface [DMS] was conducted for four regions. The YS was divided into two regions, coast zone (<50 m water depth) and central zone (≥50 m), the ECS was also divided into two areas: the inner shelf (<50 m) and the middle and outer shelf (50–200 m).

Along the YS coast, surface [DMS] as well as surface [DMSPd], were maintained at a peak level between May and September, while total surface [Chla] reached a maximum in May and obviously decreased during May and September (Fig. 6a). This seasonal mismatch between [DMS] and total [Chla] were found e.g., off the coast of southern Shandong Peninsula and the west coast of Korea during later spring and summer (Figs. 5 and 7). As for the central YS, the seasonal variations of surface [DMS] was totally in agreement with that of [DMSPd] or total [Chla]; [DMS], [DMSPd] and total [Chla] all peaked in spring and autumn, and the value of the spring peak was greater than the autumn DMS peak (Fig. 6b). Moreover, [DMS] varied considerably in the YS spatially especially the central South Yellow Sea (SYS; Fig. 5). Surface [DMS] rose rapidly from March with higher [DMS] (>8 nmol/L) occurring in the western part of the central SYS. Then, a dual-core structure (>10 nmol/L) developed; and the average [DMS] of the southern core was greater. And surface [DMS] decreased in May overall, however, [DMS] in the southeastern of central SYS increased. In June, dual-core structure disappeared entirely. Following the autumn bloom, surface [DMS] rose considerably in the eastern and southwestern park of the central SYS, and a different dual-core structure (>10 nmol/L) developed after September where average [DMS] in the east was greater as compared with that in the west. And these spatial and temporal variations were basically consistent with surface total [Chla] (Figs. 5 and 7).

Along the inner ECS shelf, both the surface [DMS] and [DMSPd] rose from early spring and reached a maximum during August, while the prominent peak of total surface [Chla] occurred in late spring (Fig. 6c). And the seasonal mismatch between surface [DMS] and total [Chla] was mainly found off the coast of Zhejiang Province during summer (Figs. 5 and 7). In the middle and outer ECS shelf, higher surface [DMS] and [DMSPd] occurred in April or summer with [DMS] that exceeded 10 nmol/L mainly occurring in the region east of the Zhoushan Islands (Table 3; Fig. 5 and 6d); however, there was totally no peak of total [Chla] in summer (Fig. 6d). During September and October, surface [DMS] maintained at a higher level (Fig. 6d), and [DMS] that went beyond 10 nmol/L were mainly found in east and southeast of the Zhoushan Islands during September, and southwest of Jeju Island and

**Table 3**
Surface dimethylsulfide concentrations (nmol/L) in selected areas.

| Regions | Annual mean | Spring (Mar. to May) | Summer (Jun. to Aug.) | Autumn (Sep. to Nov.) | Winter (Dec. to Feb.) |
|---|---|---|---|---|---|
| YECS (<200 m water depth) | 4.55 | 4.91 | 7.19 | 5.48 | 0.63 |
| YS | 6.45 | 6.85 | 9.60 | 8.37 | 0.96 |
| YS coast | 8.11 | 7.45 | 14.26 | 9.75 | 1.00 |
| central YS | 4.30 | 6.08 | 3.59 | 6.60 | 0.91 |
| ECS | 2.98 | 3.30 | 5.19 | 3.07 | 0.36 |
| inner ECS shelf | 3.98 | 3.87 | 7.35 | 3.89 | 0.82 |
| middle and outer ECS shelf | 2.57 | 3.07 | 4.30 | 2.74 | 0.17 |

YECS = the Yellow and East China seas; YS = Yellow Sea; ECS = East China Sea.

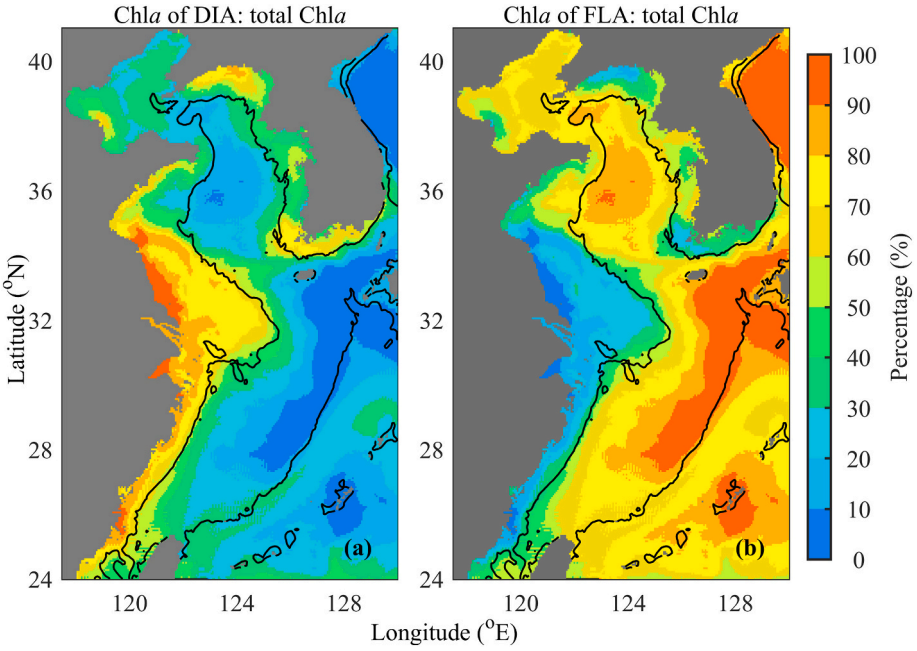


**Fig. 4.** The distribution of (**a**) the ratio of diatoms (DIA)-derived chlorophyll *a* (Chla) to total Chla and (**b**) the ratio of flagellates (FLA)-derived Chla to total Chla. Black contours denote 50 and 200 m isobaths.

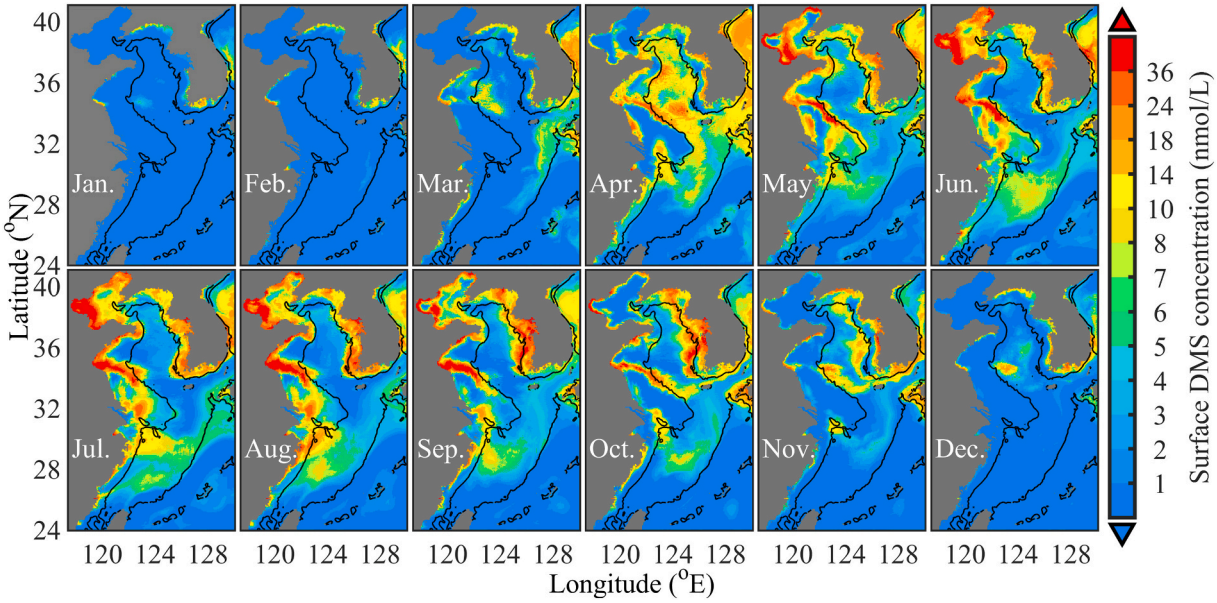


**Fig. 5.** The distribution of surface dimethylsulfide (DMS) concentrations (nmol/L). Black contours denote 50 and 200 m isobaths.

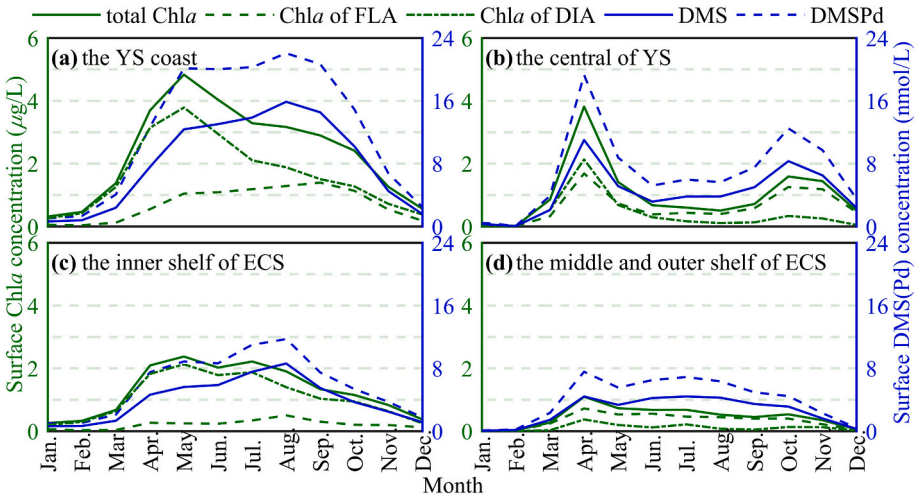


**Fig. 6.** Surface total chlorophyll *a* (Chla) concentrations (μg/L; green solid line), Chla concentrations of flagellates (FLA, μg/L; green dotted line), Chla concentrations of diatoms (DIA, μg/L; green dash dot line), dimethylsulfide (DMS) concentrations (nmol/L; blue solid line) and dissolved dimethylsulfoniopropionate (DMSPd) concentrations (nmol/L; blue dotted line) for the (**a**) Yellow Sea (YS) coast (<50 m water depth), (**b**) central YS (≥50 m), (**c**) East China Sea (ECS) inner shelf (<50 m), and (**d**) middle and outer shelf of the ECS (50–200 m). (For interpretation of the references to colour in this figure legend, the reader is referred to the web version of this article.)

east of the Zhoushan Islands during October (Fig. 5). Surface [DMS] was lower in the middle and outer ECS shelf than that along the inner shelf, and the ECS [DMS] were lower compared to those in the YS (Table 3). In total, the seasonal variations of surface [DMS] were generally consistent with that of surface total [Chla], but there were mismatches between them.

## 4. Discussions

### 4.1. Controlling factors of the annual dimethylsulfide cycle

Surface [Chla] of FLA may be an important variable to explain the mismatch between concentrations of total Chla and DMS (Fig. 6). For example, surface [DMS] as well as FLA [Chla], were maintained at a peak value along the YS coast during late summer and early autumn, while total [Chla] reduced between May and September (Fig. 6a). These results indicated that both total [Chla] and phytoplankton community structure may determine the seasonal cycle of surface [DMS] in the YECS.

Runs 1 and 2 were designed to determine how phytoplankton community affected surface [DMS]. Obviously, it can change the timing of a prominent peak; the output from Run 2 showed that the maximum monthly surface [DMS] occurred in May other than in August along the YS coast, and along the ECS coast, it peaked in July other than in August (Fig. 8a and c). However, the change of peak occurrence was not found in the central YS (Fig. 8b) suggesting that the effect size of phytoplankton community varied spatially. Fig. 9a showed the horizontal distribution of correlation coefficient (r) between monthly surface [DMS] from Runs 1 and 2. Lower r values (<0.90) were mainly found in the eastern North YS (NYS), the northern SYS, off the coast of southern Shandong Peninsula, northeast of the Zhoushan Islands, and along the Zhejiang coast, suggesting that the phytoplankton community played a crucial role on surface DMS seasonality in these sea areas.

Eliminating the influence of temperature on phytoplankton active exudation and free DMSP-lyase cleavage also changed the timing of prominent peak along the coast, furthermore, in the middle and outer shelf of ECS, surface [DMS] peaked in April and decreased during late spring and summer in Run 3 (Fig. 8). And Fig. 9b shows that lower r (<0.90) between monthly surface [DMS] from Runs 1 and 3 were mainly found in the northern NYS and the middle and outer ECS shelf. Hence,

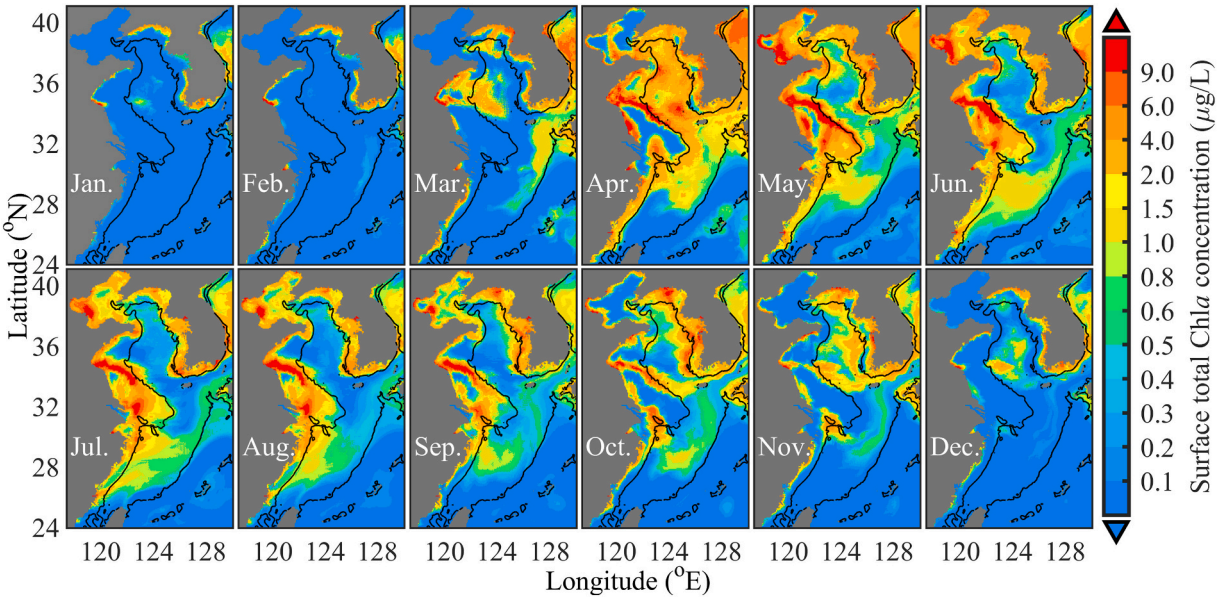


**Fig. 7.** The distribution of surface total chlorophyll *a* (Chla) concentrations (μg/L). Black contours denote 50 and 200 m isobaths.

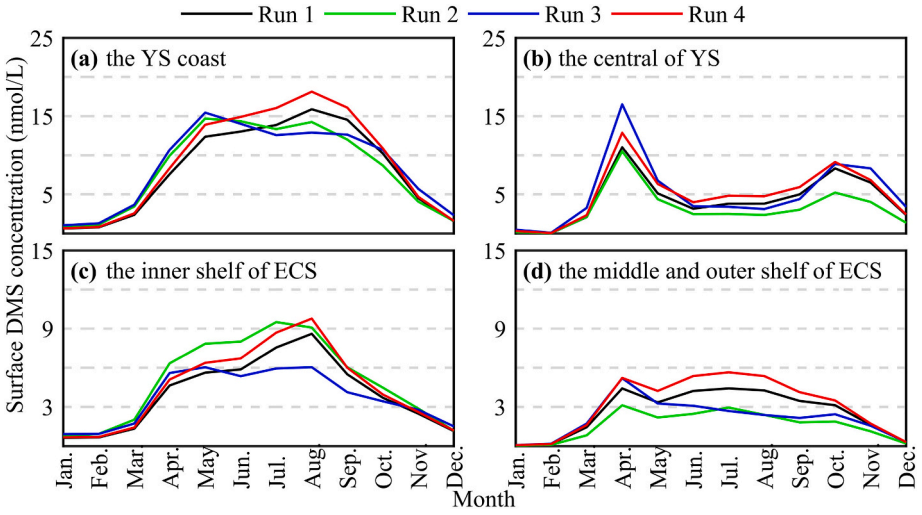


**Fig. 8.** Monthly surface dimethylsulfide (DMS) concentrations from Runs 1 (black line), 2 (green line), 3 (blue line) and 4 (red line) for the (**a**) Yellow Sea (YS) coast (<50 m water depth), (**b**) central YS (≥50 m), (**c**) East China Sea (ECS) inner shelf (<50 m), (**d**) middle and outer ECS shelf (50–200 m). (For interpretation of the references to colour in this figure legend, the reader is referred to the web version of this article.)

temperature played an important role on surface DMS seasonality in the middle and outer ECS shelf.

If we removed the photolysis term, approximately 11% of the surface [DMS] was added in the YECS, and the seasonal variations in surface [DMS] from Run 4 were in agreement with Run 1 in every selected region (Fig. 8). In addition, lower r values (<0.90) between [DMS] from Runs 1 and 4 were only found in waters east of Taiwan (not shown). However, the [DMS] elevated with a wider margin in the offshore regions compared with that in the nearshore regions. Because more light is absorbed by particles in nearshore waters, and Iz is relatively lower.

These results revealed that both the phytoplankton community and sea water temperature exerted crucial effects on seasonal variations of surface [DMS] in the YECS, but that these impacts notably varied over space.

### 4.2. Annual mean surface dimethylsulfide concentrations

The annual mean surface [DMS] in the YECS was higher than those in some other productive marginal seas which are widely studied (e.g., NW and NE Atlantic Shelves, Eastern Canary Coastal Current, NW Arabian Sea upwelling zone, North Pacific epicontinental seas), similar to the annual mean of the Humboldt Coastal Current and lower than some other water masses (e.g., Alaska Coastal Current, West India Coastal Currents; Fig. 2 exhibited by Lana et al. (2011)). In addition, the annual mean surface [DMS] or the oceanic DMS source to the atmosphere (6.78 μmol/($m^2$ day)) of the YECS from our model output was about 1.94 or 1.42 times, respectively, to the global annual mean concentrations provided by Lana et al. (2011) or the annual mean sea-to-air DMS flux given by a recent research (Wang et al., 2020), indicating that the YECS DMS emissions was not negligible.

## 5. Conclusions

We developed a three-dimensional hydrodynamic module coupled with DMS biophysical and geochemical processes for studying annual DMS cycle of the YECS and discussing its controlling factors. This model

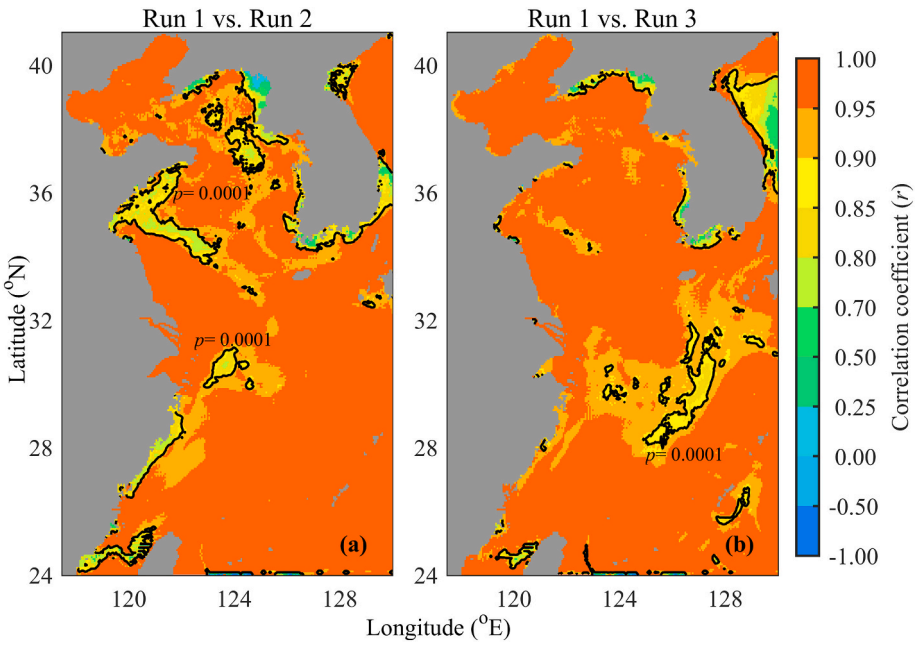


**Fig. 9.** The distribution of correlation coefficient (r) between monthly surface dimethylsulfide concentrations from (**a**) Runs 1 and 2, (**b**) Runs 1 and 3. Black contours denote isolines where the *p* value is equal to 0.0001.

reproduced spatial and seasonal variations in surface concentrations of climatologic DMS. Our main results from standard run and sensitivity experiments were as follows:

1. Surface [DMS] varied temporally and spatially in the YECS. The [DMS] peaked in summer along the coast, while there were several DMS peaks in the central YS and the middle and outer ECS shelf. In each season, surface [DMS] was higher in the nearshore regions than that in the offshore regions, and it was higher in the YS compared to that in the ECS.
2. The annual mean surface [DMS] reached to 4.55 nmol/L in the YECS, and the annual emissions of marine DMS from this area to the atmosphere arrived at 0.0705 Tg(S)/yr, accounting for 0.35% of the global oceanic DMS emissions despite this area accounting for only 0.25% of the global ocean area.
3. Seasonality of surface [DMS] was driven by phytoplankton biomass, phytoplankton community and sea water temperature; the peak month of [DMS] was affected by phytoplankton community or temperature, while photolysis mainly changed the magnitude of surface [DMS]. Moreover, effect size of phytoplankton community or temperature varied spatially.

Unsynchronized changes in nutrient levels found in Chinese coastal waters may lead to a series of ecological effects (Xin et al., 2019; Wang et al., 2021a; Wang et al., 2021b). In the future, we need to focus on the response of surface [DMS] to the altered nutrient level in the YECS.

## CRediT authorship contribution statement

**Jia-Wei Shen:** Conceptualization, Data curation, Visualization, Writing – original draft. **Liang Zhao:** Conceptualization, Methodology, Writing – review & editing, Supervision. **Hong-Hai Zhang:** Investigation, Data curation. **Hao Wei:** Writing – review & editing, Supervision. **Xinyu Guo:** Writing – review & editing.

## Declaration of competing interest

The authors declare that they have no known competing financial interests or personal relationships that could have appeared to influence the work reported in this paper.

## Acknowledgements

This work was supported by the National Key Research and Development Program of China [No. 2016YFA0601301]; National Natural Science Foundation of China [No. 41876018]; the Tianjin Natural Science Foundation [No. 19JCZDJC40600]; grant from the Ministry of Education, Culture, Sports, Science and Technology, Japan (MEXT) to the project on Joint Usage/Research Center - Leading Academia in Marine and Environmental Research (LaMer). The initial wind speed at 10 m above sea surface was obtained from ERA-Interim (https://www.ecmwf.int/en/forecasts/datasets/reanalysis-datasets/era-interim).

## Appendix A. Supplementary data

Supplementary data to this article can be found online at https://doi.org/10.1016/j.marpolbul.2021.112517.

## References

Allen, J.I., Somerfield, P.J., Gilbert, F.J., 2007. Quantifying uncertainty in high-resolution coupled hydrodynamic-ecosystem models. J. Mar. Syst. 64 (1), 3–14.
Archer, S.D., Gilbert, F.J., Nightingale, P.D., Zubkov, M.V., Taylor, A.H., Smith, G.C., Burkill, P.H., 2002. Transformation of dimethylsulphoniopropionate to dimethyl sulphide during summer in the North Sea with an examination of key processes via a modelling approach. Deep-Sea Res. II Top. Stud. Oceanogr. 49 (15), 3067–3101.
Bopp, L., Boucher, O., Aumont, O., Belviso, S., Dufresne, J.L., Mai, P., Monfray, P., 2004. Will marine dimethylsulfide emissions amplify or alleviate global warm. Can. J. Fish. Aquat. Sci. 61 (5), 826–835.
Charlson, R.J., Lovelock, J.E., Andreae, M.O., Warren, S.G., 1987. Oceanic phytoplankton, atmospheric sulphur, cloud albedo and climate. Nature 326 (6114), 655–661.
Dabrowski, T., Lyons, K., Berry, A., Cusack, C., Nolan, G.D., 2014. An operational biogeochemical model of the north-east Atlantic: model description and skill assessment. J. Mar. Syst. 129, 350–367.
Fiddes, S., Woodhouse, M.T., Nicholls, Z., Lane, T.P., Schofield, R., 2018. Cloud, precipitation and radiation responses to large perturbations in global dimethyl sulfide. Atmos. Chem. Phys. 18 (14), 10177–10198.
Gabric, A.J., Matrai, P.A., Vernet, M., 1999. Modelling the production and cycling of dimethylsulphide during the vernal bloom in the Barents Sea. Tellus Ser. B Chem. Phys. Meteorol. 51 (5), 919–937.
Gabric, A.J., Simó, R., Cropp, R., Hirst, A.C., Dachs, J., 2004. Modeling estimates of the global emission of dimethylsulfide under enhanced greenhouse conditions. Glob. Biogeochem. Cycles 18 (2), GB2014.

Gao, N., Yang, G.P., Zhang, H.H., Liu, L., 2017. Temporal and spatial variations of three dimethylated sulfur compounds in the Changjiang estuary and its adjacent area during summer and winter. Environ. Chem. 14 (3), 160–177.
Geider, R.J., MacIntyre, H.L., Kana, T.M., 1998. A dynamic regulatory model of phytoplanktonic acclimation to light, nutrients, and temperature. Limnol. Oceanogr. 43 (4), 679–694.
Grandey, B.S., Wang, C., 2015. Enhanced marine Sulphur emissions offset global warming and impact rainfall. Sci. Rep. 5, 13055.
Guo, X., Hukuda, H., Miyazawa, Y., Yamagata, T., 2003. A triply Nested Ocean model for simulating the Kuroshio—roles of horizontal resolution on JEBAR. J. Phys. Oceanogr. 33 (1), 146–169.
Gypens, N., Borges, A.V., 2014. Increase in dimethylsulfide (DMS) emissions due to eutrophication of coastal waters offsets their reduction due to ocean acidification. Front. Mar. Sci. 1 (4), 1–6.
Gypens, N., Borges, A.V., Speeckaert, G., Lancelot, C., 2014. The dimethylsulfide cycle in the Eutrophied Southern North Sea: a model study integrating phytoplankton and bacterial processes. PLoS One 9 (1), e85862.
Hao, Q., Chai, F., Xiu, P., Bai, Y., Chen, J.F., Liu, C.G., Le, F.F., Zhou, F., 2019. Spatial and temporal variation in chlorophyll a concentration in the Eastern China Seas based on a locally modified satellite dataset. Estuar. Coast. Shelf Sci. 220, 220–231.
Jian, S., Zhang, H.H., Zhang, J., Yang, G.P., 2018. Spatiotemporal distribution characteristics and environmental control factors of biogenic dimethylated sulfur compounds in the East China Sea during spring and autumn. Limnol. Oceanogr. 63 (S1), S280–S298.
Keller, M.D., Bellows, W.K., Guillard, R.R.L., 1989. Dimethyl sulfide production in marine phytoplankton. In: Saltzman, E., Cooper, W. (Eds.), Biogenic Sulfur in the Environment. American Chemical Society, Washington, DC, pp. 167–182.
Kettle, A.J., Andreae, M.O., Amouroux, D., Andreae, T.W., Bates, T.S., Berresheim, H., Bingemer, H., Boniforti, R., Curran, M.A.J., Ditullio, G.R., 1999. A global database of sea surface dimethylsulfide (DMS) measurements and a procedure to predict sea surface DMS as a function of latitude, longitude, and month. Glob. Biogeochem. Cycles 13 (2), 399–444.
Kloster, S., Feichter, J., Maier-Reimer, E., Six, K.D., Stier, P., Wetzel, P., 2006. DMS cycle in the marine ocean-atmosphere system-a global model study. Biogeosciences 3 (1), 29–51.
Kloster, S., Six, K.D., Feichter, J., Maier-Reimer, E., Roeckner, E., Wetzel, P., Stier, P., Esch, M., 2007. Response of dimethylsulfide (DMS) in the ocean and atmosphere to global warming. J. Geophys. Res. Biogeosci. 112, G03005.
Lana, A., Bell, T.G., Simó, R., Vallina, S.M., Ballabrera-Poy, J., Kettle, A.J., Dachs, J., Bopp, L., Saltzman, E.S., Stefels, J., 2011. An updated climatology of surface dimethlysulfide concentrations and emission fluxes in the global ocean. Glob. Biogeochem. Cycles 25 (1), GB1004.
Nightingale, P.D., Malin, G., Watson, A.J., Liss, P.S., Liddicoat, M.I., Boutin, J., Upstillgoddard, R.C., 2000. In situ evaluation of air-sea gas exchange parameterizations using novel conservative and volatile tracers. Glob. Biogeochem. Cycles 14 (1), 373–387.
Saltzman, E.S., King, D.B., Holmen, K., Leck, C., 1993. Experimental determination of the diffusion coefficient of dimethylsulfide in water. J. Geophys. Res. 98 (C9), 16481–16486.
Shen, J.W., Zhao, L., Wang, S.J., Li, Y.X., 2019. Multivariate analysis between dimethylsulfide and environmental factors and modeling in the Yellow Sea and the East China Sea. China Environ. Sci. 39 (6), 2514–2522.
Skogen, M.D., Søiland, H., 1998. A user's guide to NORWECOM v2.0, a coupled 3 dimensional physical chemical biological ocean-model. In: the NORWegian ecological model system. Bergen, Institute of Marine Research, Technical Report Fisken og Havet 18/98 available online at: http://www.imr.no/morten/norwecom/userguide2_0.ps.gz.
Speeckaert, G., Borges, A.V., Champenois, W., Royer, C., Gypens, N., 2018. Annual cycle of dimethylsulfoniopropionate (DMSP) and dimethylsulfoxide (DMSO) related to phytoplankton succession in the Southern North Sea. Sci. Total Environ. 622–623, 362–372.
Stefels, J., Steinke, M., Turner, S., Malin, G., Belviso, S., 2007. Environmental constraints on the production and removal of the climatically active gas dimethylsulphide (DMS) and implications for ecosystem modelling. Biogeochemistry 83 (1–3), 245–275.
Sun, D.Y., Huan, Y., Wang, S.Q., Qiu, Z.F., Ling, Z.B., Mao, Z.H., He, Y.J., 2019a. Remote sensing of spatial and temporal patterns of phytoplankton assemblages in the Bohai Sea, Yellow Sea, and East China Sea. Water Res. 157, 119–133.
Sun, X.R., Shen, F., Brewin, R., Liu, D.Y., Tang, R.G., 2019b. Twenty-year variations in satellite-derived chlorophyll-a and phytoplankton size in the Bohai Sea and Yellow Sea. J. Geophys. Res. Oceans 124 (12), 8887–8912.
Vogt, M., Vallina, S.M., Buitenhuis, E.T., Bopp, L., Quere, C.L., 2010. Simulating dimethylsulphide seasonality with the dynamic Green Ocean model PlankTOM5. J. Geophys. Res. Oceans 115, C06021.
Wang, J., Bouwman, A.F., Liu, X., Beusen, A.H.W., Van Dingenen, R., Dentener, F., Yao, Y., Glibert, P.M., Ran, X., Yao, Q., Xu, B., Yu, R., Middelburg, J.J., Yu, Z., 2021a. Harmful algal blooms in Chinese coastal waters will persist due to perturbed nutrient ratios. Environmental Science & Technology Letters 8 (3), 276–284.
Wang, Q., Guo, X., Takeoka, H., 2008. Seasonal variations of the Yellow River plume in the Bohai Sea: a model study. J. Geophys. Res. Oceans 113, C08046.
Wang, W.-L., Song, G.-S., Primeau, F.W., Saltzman, E.S., Moore, J.K., 2020. Global ocean dimethyl sulfide climatology estimated from observations and an artificial neural network. Biogeosciences 17, 5335–5354.
Wang, Y., Xu, H., Li, M., 2021b. Long-term changes in phytoplankton communities in China's Yangtze Estuary driven by altered riverine fluxes and rising sea surface temperature. Geomorphology 376, 107566.
Wang, Y.C., Guo, X., Zhao, L., Zhang, J., 2019. Seasonal variations in nutrients and biogenic particles in the upper and lower layers of East China Sea shelf and their export to adjacent seas. Prog. Oceanogr. 176, 102138.
Xin, M., Wang, B., Xie, L., Sun, X., Wei, Q., Liang, S., Chen, K., 2019. Long-term changes in nutrient regimes and their ecological effects in the Bohai Sea, China. Mar. Pollut. Bull. 146, 562–573.
Xu, F., Jin, N., Ma, Z., Zhang, H.H., Yang, G.P., 2019. Distribution, occurrence, and fate of biogenic dimethylated sulfur compounds in the Yellow Sea and Bohai Sea during spring. J. Geophys. Res. Oceans 124 (8), 5787–5800.
Yang, G.P., Zhang, H.H., Zhou, L.M., Yang, J., 2011. Temporal and spatial variations of dimethylsulfide (DMS) and dimethylsulfoniopropionate (DMSP) in the East China Sea and the Yellow Sea. Cont. Shelf Res. 31 (13), 1325–1335.
Yang, G.P., Song, Y.Z., Zhang, H.H., Li, C.X., Wu, G.W., 2014. Seasonal variation and biogeochemical cycling of dimethylsulfide (DMS) and dimethylsulfoniopropionate (DMSP) in the Yellow Sea and Bohai Sea. J. Geophys. Res. Oceans 119 (12), 8897–8915.
Zhai, X., Li, J.L., Zhang, H.H., Tan, D.D., Yang, G.P., 2019. Spatial distribution and biogeochemical cycling of dimethylated sulfur compounds and methane in the East China Sea during spring. J. Geophys. Res. Oceans 124 (2), 1074–1090.
Zhang, J., Guo, X., Zhao, L., 2019. Tracing external sources of nutrients in the East China Sea and evaluating their contributions to primary production. Prog. Oceanogr. 176, 102122.
Zhao, L., Guo, X., 2011. Influence of cross-shelf water transport on nutrients and phytoplankton in the East China Sea: a model study. Ocean Sci. 7 (1), 27–43.
Zhu, R., Yang, G.P., Zhang, H.H., 2019. Temporal and spatial distributions of carbonyl sulfide, dimethyl sulfide, and carbon disulfide in seawater and marine atmosphere of the Changjiang estuary and its adjacent East China Sea. Limnol. Oceanogr. 64 (2), 632–649.